Construction of Time-Dependent Spectra Using Wavelet Analysis for Determination of Global Damage

Micaletti, R. C.; Cakmak, A. S.; Nielsen, Søren R.K.; Kirkegaard, Poul Henning

Publication date:
1995

Document Version
Publisher's PDF, also known as Version of record

INSTITUTTET FOR BYGNINGSTEKNIK

DEPT. OF BUILDING TECHNOLOGY AND STRUCTURAL ENGINEERING
AALBORG UNIVERSITET • AUC • AALBORG • DANMARK

STRUCTURAL RELIABILITY THEORY
PAPER NO. 147

To be presented at the Noise and Vibration Engineering Conference, Leuven, Belgium, September 1996

R. C. Micaletti, A. Ş. Çakmak, S. R. K. Nielsen & P. H. Kirkegaard

CONSTRUCTION OF TIME-DEPENDENT SPECTRA USING WAVELET ANALYSIS FOR DETERMINATION OF GLOBAL DAMAGE

JULY 1995 ISSN 0902-7513 R9517

Printed at Aalborg University

INSTITUTTET FOR BYGNINGSTEKNIK
DEPT. OF BUILDING TECHNOLOGY AND STRUCTURAL ENGINEERING
AALBORG UNIVERSITET • AUC • AALBORG • DANMARK

STRUCTURAL RELIABILITY THEORY
PAPER NO. 147

To be presented at the Noise and Vibration Engineering Conference, Leuven, Belgium, September 1996

R. C. Micaletti, A. Ş. Çakmak, S. R. K. Nielsen & P. H. Kirkegaard

CONSTRUCTION OF TIME-DEPENDENT SPECTRA USING WAVELET ANALYSIS FOR DETERMINATION OF GLOBAL DAMAGE

JULY 1995 ISSN 0902-7513 R9517

Construction of Time-Dependent Spectra Using Wavelet Analysis for Determination of Global Damage

R.C. Micaletti, A.S. Cakmak
Department of Civil Engineering and Operations Research, Princeton University, Princeton, NJ 08544, USA

and

S.R.K. Nielsen, P.H. Kirkegaard
Department of Building Technology and Structural Engineering, Aalborg University, DK-9000 Aalborg, Denmark

Abstract
A new method for computing the Maximum Softening Damage Index (MSDI) is proposed. The MSDI, a measure of global damage, is based on the relative reduction of the first eigenfrequency (or equivalently, the relative increase in the fundamental period) of a structure over the course of a damaging event. The method proposed here makes use of wavelet transform coefficients of measured output response records to provide time-localized information on structural softening. A time-dependent Fourier transform is derived which provides better frequency resolution at low-to-mid-range frequencies than standard windowed Fourier transform analysis while still providing reasonable estimates of time-localized spectral content. The method is applied to real data taken from tests conducted at the University of Illinois at Urbana-Champaign on a model 10-story reinforced-concrete structure [1]. Results from the proposed method are compared with results from a previously proposed method known as the Moving Window Transfer Function method. The new method is found to produce comparable estimations of the MSDI with the potential for increased efficiency over the MWTF method.

1 Introduction

The Maximum Softening Damage Index is a measure of global damage proposed by Dipasquale and Cakmak [3] for seismic analysis of real structures. Of the three categories of damage indices [9], empirically-based, energy-based, and vibrationally-based, the MSDI falls into the last category with its theoretical basis derived from continuum damage mechanics [4]. Correlations between actual damage levels and damage levels computed with the MSDI have been demonstrated through seismic assessment of actual strong-motion records from medium-rise reinforced-concrete (RC) structures subjected to the 1971 San Fernando earthquake [3]. Dipasquale and Cakmak have defined the MSI as

$$\delta_m = 1 - \frac{T_0}{T_{max}} \tag{1}$$

where T_0 is the initial undamaged fundamental period of the structure and T_{max} is the maximum fundamental period of the time-varying equivalent linear structure based on the assumption that the B actual nonlinear structure can be represented as a slowly-varying linear structure within a small time window. As is evident, the definition of the MSDI states that a simple relationship exists between the damage intensity as measured by the index and the ratio of the undamaged to maximum fundamental periods. Indeed this simplicity is one of the two main advantages that the MSDI has over other measures of global damage [9]. The other main advantage is that the MSDI can be computed solely from measured input/output records.

Though the definition of the MSDI is simple and straightforward, reliable computation of the MSDI has proved to be somewhat difficult. The determination of the variation over time of the fundamental period (or equivalently, fundamental frequency) of the structure from measured data requires time-localized information of the frequency content of the output response (and possibly the input accelerations). The need for time-localized frequency information is a standard problem encountered in signal processing. As such, classical signal processing methods have been employed in the computation of the MSDI.

One such method, known as the Moving Window Transfer Function method (MWTF) [6], employs standard Fourier transform analysis on overlapping windows (where the structure is assumed to behave linearly) of the measured input acceleration and output response records to produce time-localized (windowed) power spectra. From the windowed input and output power spectra, empirical transfer functions are computed in accordance with linear random vibration theory. The frequencies at which the peaks of the transfer function occur are taken as the eigenfrequencies of the structure at the time-center of the window. In this manner, the evolution of the fundamental period can be traced and its maximum value identified.

The development of the MWTF method was motivated by the desire to have a means of computing the MSDI that met the following objectives [6]:

1. Ability to compute frequency variations from data without recourse to a specific dynamic model of the system.
2. Require little or no user input.
3. Require little or no user feedback.
4. Computational efficiency
5. Ability to produce a reliable estimate of the MSI

Implementation of the MWTF method has shown that it essentially meets objectives 1-3 and 5 [6]. However, due to excessive FFT computations caused by the use of overlapping windows, the MWTF does not meet the objective of computational efficieny. In addition, the MWTF method does require some user input and feedback which directly influence the estimate of the MSDI.

In this paper, we propose a new approach for computing the MSDI that meets the criteria set forth above. The approach is based on the construction of time-dependent Fourier transforms of a structure's output response time-history. These time-dependent Fourier transforms are composed of linear combinations of wavelet Fourier transforms weighted by time-localized and frequency-localized wavelet coefficients. The eigenfrequencies of the structure are taken as the peaks of the time-dependent Fourier amplitude spectra of the output response under the assumption that the spectra of the input accleration can be modeled as white-noise. This assumption precludes the possibility of obtaining spurious eigenfrequencies from empirical transfer functions due to near-zero input spectra values.The MSDI can then be evaluated by measuring the change in the first eigenfrequency of the structure over the course of the record.

2 Wavelet Analysis

Wavelet analysis has been the subject of intense mathematical research for the past decade [2]. Although its origins can be traced to the early part of the 20th century, its recent revival in the early 1980's stems from the analysis of seismic signals in geophysical engineering [5]. Since this time, wavelet analysis has become a powerful tool in signal processing for its ability to provide time-localized as well as frequency-localized information about nonstationary signals of finite energy.

The continuous wavelet transform is defined as

$$(T^{wav}_{a,b} f) = \frac{1}{\sqrt{a}} \int_{-\infty}^{\infty} f(t)\psi(\frac{t-b}{a})dt \tag{2}$$

In light of Eq.(2), the wavelet transform can be viewed as a projection of the function $f(t)$ onto the basis $\psi(\frac{t-b}{a})$ where $\psi(t)$ is the wavelet, a is the dilation parameter, and b is the translation parameter. The parameters a and b serve to provide the dual localization of the wavelet in both time and frequency. However, due to the uncertainty principle, it is impossible to obtain equally high resolution in time and frequency simultaneously. For this reason, the parameter b is dependent on the parameter a. At high values of a, the wavelet is wide and extends over a large interval in the time domain, consequently, its Fourier transform is concentrated on a small interval in the frequency domain. This corresponds to poor time-localization and high frequency resolution. At small values of a the situation is reversed, the wavelet is compact in the time domain and, therefore, its Fourier transform is dilated. This corresponds to good localization in time and poor resolution in frequency. For mid-range values of a, moderate resolution in both time and frequency is achieved.

Though there are many wavelets from which to choose, in this paper we use a Daubechies [2], [8] wavelet defined as follows,

$$\psi(t) = \sum_{k=0}^{M-1} (-1)^{k+1} c_{M-k-1}\phi(t-k) \tag{3}$$

where

$$\phi(t) = \sum_{k=0}^{M-1} c_k \phi(2t-k) \tag{4}$$

$\phi(t)$ is called a scaling function and it is generated iteratively by Eq.(4) which is known as a dilation equation. A convenient starting point for $\phi(t)$ is the indicator function on the unit interval $[0,1]$, i.e.,

$$\phi(t) = \begin{cases} 1 & \text{if } t \in [0,1] \\ 0 & \text{otherwise} \end{cases} \tag{5}$$

The coefficients c_k represent filter coefficients. It should be noted that any even number M of filter coefficients can be used as long as they meet certain accuracy and orthogonality conditions

[8]. The more filter coefficents that are used, the more regular and continuously differentiable the wavelet becomes (also, its Fourier amplitude spectrum becomes more concentrated on a narrower frequency band) [2]. Using two filter coefficients, a superposition of wavelets can exactly represent a polynomial of degree one. Each increase by two of filter coefficients allows one to exactly represent a polynomial of one higher degree. For the purposes of this paper, we use 10 Daubechies filter coefficients. The function $\psi(t)$ in Eq.(3), known as the "mother" wavelet, is generated by reversing the order and alternating the signs of the filter coefficients in Eq.(4). A pleasant characteristic of the Daubechies wavelets is the orthonormality between dilates and translates of $\psi(t)$ [2]. This orthonormality of the Daubechies wavelet enables any signal of finite energy to be expressed as a linear combination of the wavelet basis [8], i.e.,

$$f(t) = \sum_{j=-\infty}^{\infty} \sum_{k=-\infty}^{\infty} a_{j,k}\psi(2^j t - k) \tag{6}$$

where the $a_{j,k}$ are the wavelet coefficients of the expansion (similar to Fourier coefficients) and the $\psi(2^j t - k)$ are the family of wavelet functions generated by dilating and translating the function $\psi(t)$.

To determine the $a_{j,k}$ wavelet coefficients, a pyramid algorithm discovered by Mallat [7], [8] was used. To employ the algorithm, the number of data points in the signal to be analyzed, $f(t)$, must be an integer power of two, therefore, zero-padding of the data may be necessary. In addition, for ease of calculations, it is convenient to consider $f(t)$ as one period of a periodic function that spans the dimensionless unit interval $[0,1]$ and repeats itself in subsequent unit intervals [8]. With these considerations (and with 2^N data points), $f(t)$ in Eq.(6) can be written as,

$$f(x) = a_{-1,0}\phi(x) + \sum_{j=0}^{N-1} \sum_{k=0}^{2^j-1} a_{j,k}\psi(2^j x - k) \qquad x \in [0,1] \tag{7}$$

where x is now a dimensionless quantity. If the length of the record is T, then $x = \frac{t}{T}$. The first term on the right-hand side of Eq.(7) represents the contribution from all negative wavelet levels [8]. The index j represents the frequency level of the wavelet. At level j, there are 2^j wavelets in the unit interval which can be interpreted as 2^j cycles/unit interval [8]. With this interpretation, the average frequency at level j can be determined by the relation

$$freq_j = \frac{2^j f_s}{2^N} \tag{8}$$

where f_s is the sampling frequency of the data.

Note that the average frequency of an arbitrary wavelet level is the center of the frequency bandwidth traversed by the wavelets at that level. As one proceeds from level j to level $j+1$, the average frequency doubles as does the frequency bandwidth of the wavelet. Therefore, at low values of j, the frequency bandwidth is relatively narrow and good frequency resolution results, at the expense of time-localization. At high values of j, the frequency bandwidth is rather wide resulting in less frequency resolution, consequently, the time-localization is greater. (Essentially this is true, though because the Daubechies wavelets are compact in the time domain, their Fourier transforms extend over the entire frequency axis. However, these Fourier transforms are negligible outside a finite frequency interval, the length of which depends on the frequency level.)

The index k denotes the number of translations of a jth-level wavelet that are needed to cover the unit interval. As stated above, there are 2^j wavelets in the unit interval, therefore, each wavelet corresponds to an interval of time of length $\frac{T}{2^j}$. In light of this, each wavelet coefficient $a_{j,k}$ expresses the significance of the projection of $f(t)$ onto the wavelet at frequency level j and time interval k. A large value for an arbitrary $a_{j,k}$ implies that during the kth time interval, the frequency content of $f(t)$ lies within the frequency band spanned by the jth-level wavelet.

3 Spectral Estimation Using Wavelets

As mentioned in the introduction, in order to determine the MSDI, time-localized frequency information is needed to trace the evolution of the fundamental period of the structure. To this end, taking the Fourier transform of both sides of Eq.(7) results in,

$$\int_{-\infty}^{\infty} f(x)e^{-i\omega x}dx = \int_{-\infty}^{\infty}\{a_{-1,0}\phi(x) + \sum_{j=0}^{N-1}\sum_{k=0}^{2^j-1} a_{j,k}\psi(2^j x - k)\}e^{-i\omega x}dx \tag{9}$$

Denoting the Fourier transform of an arbitrary function, $g(x)$, as $\hat{g}(\omega)$, Eq.(9) simplifies to

$$\hat{f}(\omega) = a_{-1,0}\hat{\phi}(\omega) + \sum_{j=0}^{N-1}\sum_{k=0}^{2^j-1} a_{j,k}e^{-i\frac{\omega}{2^j}k}\frac{1}{2^j}\hat{\psi}(\frac{\omega}{2^j}) \tag{10}$$

where the term $\frac{1}{2^j}\hat{\psi}(\frac{\omega}{2^j})$ is a dilated version of $\hat{\psi}(\omega)$ and represents the Fourier transform of the jth-level wavelet. The term $e^{-i\frac{\omega}{2^j}k}$ is necessary to account for the phase-shifts of the translated versions of $\psi(2^j x)$.

Since the index k contains the time-localization information, in order to construct a time-localized Fourier transform, it is necessary to interchange the order of summation in Eq.(10). To do this, the inner summation must be made independent of j. At the uppermost j-level there are 2^{N-1} intervals indexed by k, therefore, to remove the dependence on j of the inner summation, it is necessary to artificially subdivide the k-intervals at each j-level such that every level contains 2^{N-1} intervals. Figure (1) illustrates this concept. Correspondingly, the $a_{j,k}$ values must then be distributed in such a manner over the subintervals of the respective k-intervals so that the total summation remains the unchanged. Here the $a_{j,k}$ values are distributed equally over the subintervals which is equivalent to assuming stationarity of the response over a small time window. This can be written as

$$\hat{f}(\omega) = a_{-1,0}\hat{\phi}(\omega) + \sum_{k'=0}^{2^{N-1}-1}\sum_{j=0}^{N-1} \frac{\tilde{a}_{j,k'}}{2^{N-1-j}}e^{-i\frac{\omega}{2^j}\lfloor\frac{k'}{2^{N-1-j}}\rfloor}\hat{\psi}(\frac{\omega}{2^j}) \tag{11}$$

where $\lfloor\frac{k'}{2^{N-1-j}}\rfloor$ signifies the integer part of the argument and

$$\tilde{a}_{j,k'} = a_{j,\lfloor\frac{k'}{2^{N-1-j}}\rfloor}$$

These modifications are needed to ensure that the right-hand sides of Eqs.(10) and (11) remain equal.

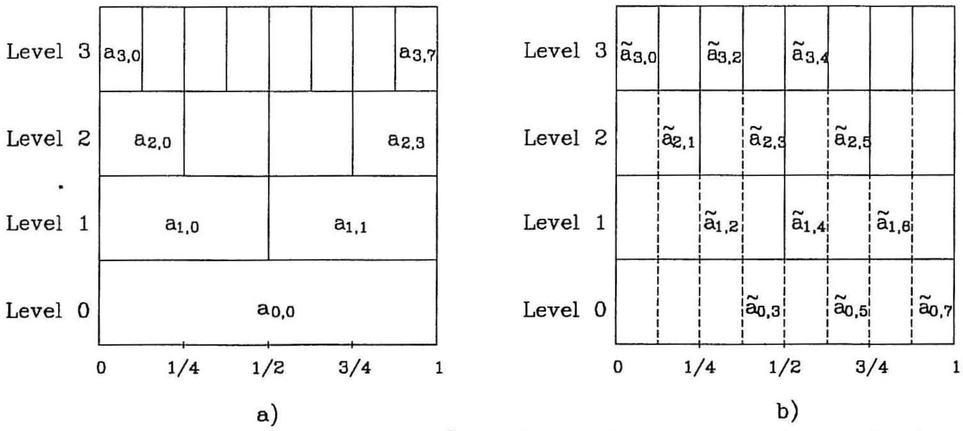

Figure 1: *For an input sequence of* $2^4 = 16$ *points, there are 4 wavelet levels. Diagram (a) shows the initial hierarchy of wavelet coefficients. The* $a_{j,k}$ *represent the "information content" [2] at wavelet level* j *during dimensionless time interval* k *(represented by the length of the box). Diagram (b) shows the artificial partitioning of the wavelet levels needed to create* 2^{N-1} *wavelet coefficients at each wavelet level.*

At this point, we define the time-dependent Fourier transform centered at the time $t = \frac{k'}{2^{N-1}}T$, where T is the total duration of the record, as

$$\hat{f}(\omega, k') = \sum_{j=0}^{N-1} \frac{\tilde{a}_{j,k'}}{2^{N-1-j}} e^{-i\frac{\omega}{2^j}\lfloor\frac{k'}{2^{N-1-j}}\rfloor} \hat{\psi}(\frac{\omega}{2^j}) \tag{12}$$

such that

$$\hat{f}(\omega) = a_{-1,0}\hat{\phi}(\omega) + \sum_{k'=0}^{2^{N-1}-1} \hat{f}(\omega, k') \tag{13}$$

Eq.(12) states that the Fourier transform of the analyzed signal at the "time" k', or rather during the k'th time interval of length $\frac{T}{2^{N-1}}$, is composed of a linear combination of the Fourier transforms of the wavelets from all frequency levels (indexed by j). The weights of the linear combination are the modified $\tilde{a}_{j,k'}$ coefficients, which express the relative contribution of wavelets from level j during the time interval k'. As mentioned before, if the $\tilde{a}_{j,k'}$ coefficients are distributed equally over the k'-subintervals of the respective k-interval, this is equivalent to assuming that the wavelet at level j and interval k contributes equally over the artificial k'-subintervals of interval k, i.e., the assumption of stationarity over the respective k-interval.

4 Application and Interpretation of Time-Dependent Spectra

In order to apply Eq.(12), numerical values for the $\hat{\psi}(\frac{\omega}{2^j})$ are needed. These values can be computed by means of an inverse application of Mallat's pyramid algorithm [8]. To create a wavelet at level j, it is necessary to construct a vector of length 2^N (the same length as the analyzed data) which contains all zeros except for the $(2^j + 1)$th element which is set equal to

1. This vector then serves as the input to the inverse pyramid algorithm, the numerical output, also of length 2^N, is a jth-level wavelet. Proceeding in such a manner, wavelets from each level can be constructed and their Fourier transforms calculated.

Once the $\hat{\psi}(\frac{\omega}{2^j})$ have been computed, Eq.(12) can be applied to determine the $\hat{f}(\omega, k')$. From these time-dependent Fourier transforms, the time-dependent Fourier spectra can be calculated. With a signal of length 2^N, there will be 2^{N-1} time-dependent, spectra, which can be averaged or smoothed to varying degrees simply by adding several consecutive time-dependent transforms together, since the sum over all k' of the time-dependent transforms is the time-averaged Fourier transform of the nonstationary signal. After the spectra have been smoothed, the variation of the first eigenfrequency over time can be determined, and the MSDI computed.

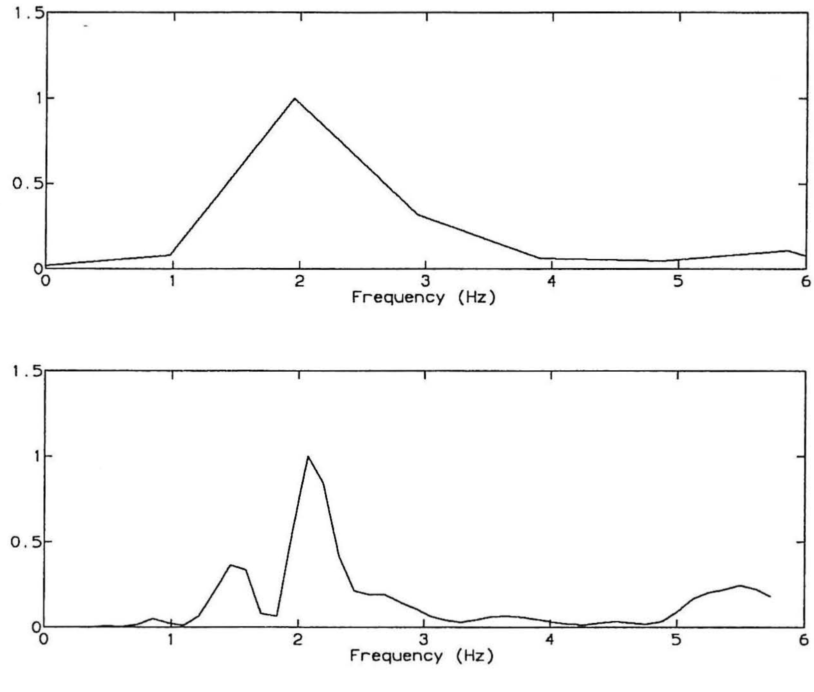

Figure 2: *The upper plot shows the windowed Fourier amplitude spectrum of the first 256 points of the Run 1 time-series. The lower plot shows the smoothed time-dependent spectrum corresponding to the same time interval of the original Run 1 time-series. Notice how the windowed Fourier spectrum smears the spectral peaks in the low frequency range.*

Since the time-dependent Fourier transform, as defined by Eq.(12), is a linear combination of the $\hat{\psi}(\frac{\omega}{2^j})$ and these $\hat{\psi}(\frac{\omega}{2^j})$ are the Fourier transforms of vectors of length 2^N, the $\hat{f}(\omega, k')$ will necessarily have higher frequency resolution than windowed Fourier transforms on segments of the data of length 2^n, where $n < N$. The uncertainty principle is not circumvented, however, as the $\hat{\psi}(\frac{\omega}{2^j})$ are the averaged spectral content of the wavelets. Nonetheless, at low-to-moderate frequency levels, which encompass the frequency range of interest to structural engineers, the averaged spectral content of the wavelets is reasonably concentrated in the frequency domain. The validity of Eq.(12) as a useful means of time-frequency analysis then rests on the validity of the distribution of the $a_{j,k'}$ coefficients over the artificial k'-intervals at low-to-moderate frequency levels. At mid-range frequency levels, where the initial k-intervals have to be subdivided less times than at lower levels, the equal distribution of the $a_{j,k}$ coefficients over the k'-intervals is not a strong assumption. At low frequency levels, the equal distribution of the $a_{j,k}$ is a stronger assumption, one that, depending on the contribution from these wavelet levels, may lead to simply averaged Fourier spectra. Thus, Eq.(12) is most useful when the frequency content of the signal is concentrated in the mid-range wavelet levels where the spectral resolution and time-localization are both fairly concentrated. With mostly high-frequency content, spectral resolution is lost. Similarly, with primarily low-frequency content, meaningful time-localization is lost. (Note: Recall that the average frequency at a given wavelet level depends on the sampling frequency and the number of data points in the time-history.)

5 Numerical Example

The foregoing procedure was applied to measured response data taken from tests conducted at the University of Illinois at Urbana-Champaign (UIUC) on a model 10-story, 3-bay, RC structure designated H1 [1]. The tests consisted of subjecting the model structure to a series of three successive seismic excitations (labeled Run 1, Run 2, and Run 3) of increasing intensity with no restrengthening of the structure between simulations. The base accelerations were scaled versions of the 1940 El Centro earthquake and the response accelerations were measured at the top story of the structure.

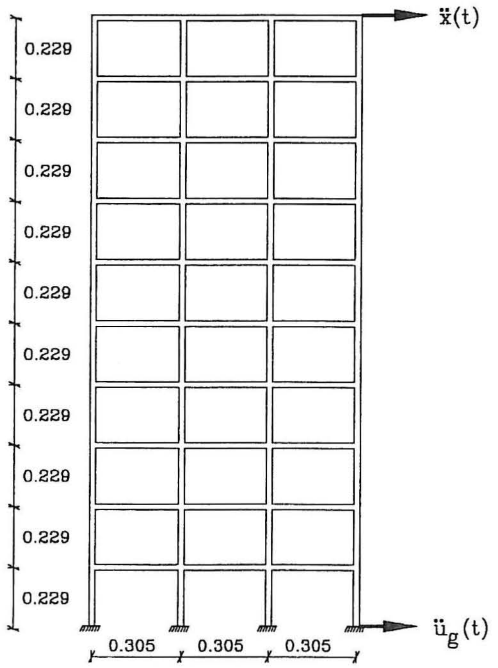

Figure 3: *Diagram of model structure tested at the University of Illinois at Urbana-Champaign. The dimensions shown are in meters.*

The three UIUC output response time-histories contained 3900 points each (at a sampling frequency of 250 Hz), however, roughly the last 500 points of each were zero. In addition, during the initial portion of each record (approximately 250 data points), the signal-to-noise ratio was quite low. By eliminating the zero-padded values and beginning the analysis during the strong-motion portion of the records, approximately 3000 data points remained in each record from which to extract meaningful eigenfrequency estimations. In order to perform wavelet analysis, the remaining data points were broken up into segments of 2048 and 1024 points. Applying Mallat's pyramid algorithm to each segment separately produced two vectors of wavelet coefficients which were in turn used (again, separately) in the application of Eq.(12). The record segments which contained 2048 points produced 1024 time-dependent spectra and similarly, the segments which contained 1024 points produced 512 time-dependent spectra. To smooth the spectra, series of 128 consecutive, non-overlapping spectra were added together. Thus, for the segments containing 2048 points and producing 1024 time-dependent spectra, there were 8 smoothed time-dependent spectra estimates, while for the record segments of 1024 points (which produced 512 time-dependent spectra) there were 4 smoothed time-dependent specta estimates, thereby producing 12 smoothed time-dependent spectra estimations for each of the three time-histories.

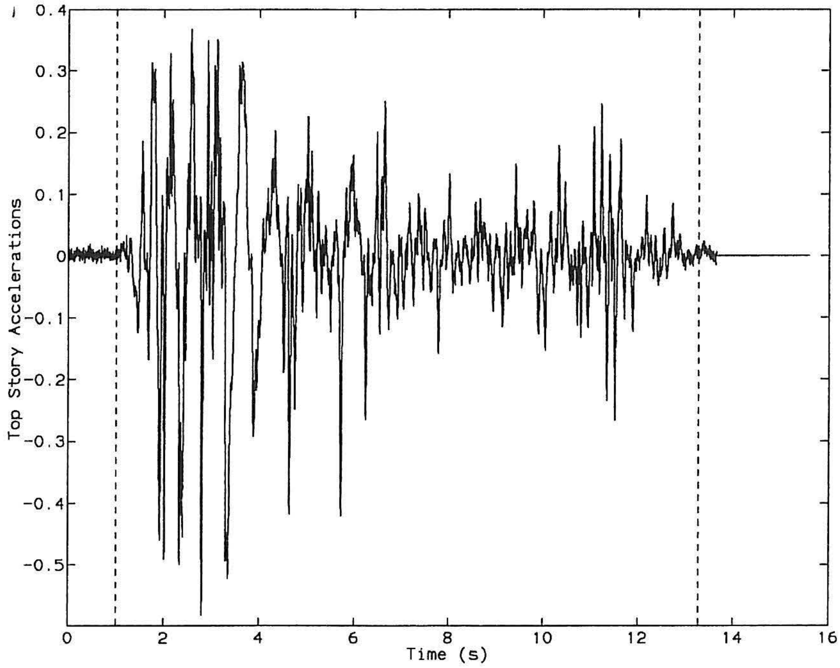

Figure 4: *Output response time-history from the first seismic simulation. The dotted lines indicate the portion of the record that was analyzed.*

In order to establish a baseline from which the reduction of the fundamental frequency could be measured, the frequency of the left-most peak in the first smoothed spectra of the first time-history was taken as the initial undamaged fundamental frequency. The subsequent fundamental frequencies were chosen according to the following criteria: they corresponded to the maximum spectral peaks whose frequencies were less than or equal to the initial undamaged fundamental frequency and then only if their spectral peaks were at least 10% of the maximum spectral peaks of their respective smoothed time-dependent spectra. The last condition was implemented to eliminate the designation of insignificant peaks as fundamental frequencies.

The following table shows the results of MSDI computations for the three UIUC time-histories using both the time-dependent spectra method (TDS) and the MWTF method.

test	TDS			MWTF		
	I.F.	M.F.	MSDI	I.F.	M.F.	MSDI
Run 1	1.709	.731	.571	2.048	1.024	.500
Run 2		.610	.643		.768	.625
Run 3		.610	.643		.512	.750

Table 1: *MSDI results for the UIUC data.*

I.F.=Initial Undamaged Frequency
M.F.=Minimum Frequency

The results for the first two cases are comparable. For the third case, the MWTF method computed a damage level of .750 while the TDS method detected no further softening of the first mode of the structure. One explanation for the discrepancy is the fact that the MWTF procedure computes empirical transfer functions by dividing the windowed output power spectra by the corresponding windowed input power spectra. As the damage level of the model structure increased, more spectral energy was concentrated at higher frequencies (observed in both Fourier and wavelet analysis) as opposed to the fundamental frequency range, indicating that the structure was being excited in higher modes. The left-most peaks of the transfer functions, whose frequencies were taken as the first eigenfrequencies, were quite likely to have been caused by near-zero input spectra values rather than being true eigenfrequencies. Thus, the MSDI value of .750 as calculated by the MWTF method may have been an overestimation of the damage level.

Alternatively, the damage index of.750 may otherwise be attributed to the limited frequency resolution of the MWTF method which relies on windowed Fourier analysis. as the initial undamaged fundamental frequencies determined by both methods and the final minimum frequencies were relatively comparable. In either case, the time-dependent/windowed Fourier spectra of the third time-history displayed very little spectral energy in the fundamental frequency range, thereby making it difficult to reliably assess the damage of the structure by means of the one-mode MSDI definition in Eq.(1). For cases such as these, relative reductions in higher modes of the structure must be taken into account as well.

One possible advantage of the TDS method over the MWTF method is the potential for increased computational efficiency. The MWTF method uses overlapping windowed Fourier analysis of input acceleration as well as output response. Multiple Fourier transforms (via FFTs) have to be computed throughout the procedure with the computational resources required increasing with the number of data points in the measured record. In contrast, the TDS method calculates the Fourier transforms of the j-level wavelets only once and then determines the time-dependent Fourier transforms as linear combinations of these wavelet Fourier transforms. In addition, the sum in Eq.(12) can be truncated such that wavelet levels with negligible contribution to the construction of the signal can be eliminated. Moreover, $\hat{f}(\omega, k')$ only has to be calculated for the range of frequencies of interest (which is case-specific) which may further reduce the computation time. However, if the signal has contributions from many wavelet levels and, in turn, the $\hat{f}(\omega, k')$ have to be computed over a large frequency range, then the TDS method is just as inefficient, if not moreso than the MWTF method.

One definite advantage of the TDS method is the increased frequency resolution at low-to-mid-range frequencies that results due to the fact that the wavelets have 2^N data points, whereas any windowed Fourier analysis will necessarily have less than 2^N data points in any time-window. Information about time-localization is not completely lost, however, as the $\tilde{a}_{j,k'}$ coefficients still express time-dependent contributions from the various wavelet levels (under the interval stationarity assumptions).

Another primary advantage the TDS method has over the MWTF method is the facility with which the TDS method can be automated for damage assessment. (In this manner, the TDS method makes it possible to meet the criteria set forth in the introduction which motivated the development of the MWTF method.) As mentioned previously, the calculation of transfer functions in the MWTF method introduced the possibility of spurious peaks due to near-zero input spectra values. To counter this, the input spectra can be filtered such that values below a specified cutoff value are ignored. This filtering can effectively eliminate most spurious peaks. However, the specification of a cutoff value is highly arbitrary and case-specific, thereby diminishing the automated capabilities of the MWTF method. In contrast, the TDS method eliminates the possibility of obtaining spurious peaks by considering the input as white-noise. This characteristic allows the TDS method to proceed in an automated fashion without the need for user input (other than the output response) or user feedback (of course, the user must still assess the reasonableness of the results). Thus, the primary limitations of the TDS method stem from the limitations in the measured data itself, e.g. excessive noise, low sampling frequency, not enough data points, highly nonstationary behavior, etc.

6 Conclusions

A time-frequency estimation technique based on wavelet analysis is proposed as a means of calculating the MSDI for structures which have undergone a damaging event. The procedure incorporates wavelet coefficients as the weights in a linear combination of wavelet Fourier transforms to produce time-dependent Fourier amplitude spectra. The procedure is found to be superior to a previously-proposed technique known as the Moving Window Transfer Function (MWTF) method in regards to frequency resolution at low-to-mid-range frequencies and its capacity for automation. In addition, the proposed method has the potential to be more computationally efficient, but this must be assessed on a case-by-case basis. The application of the proposed technique requires no structural model nor does it require *a priori* knowledge of the system's parameters other than an estimation of the initial undamaged fundamental frequency in case the structure has been previously damaged. For these reasons, the proposed technique appears to be robust and potentially useful for quick, reliable damage assessment. Moreover, the proposed technique may be applicable to other time-frequency/system identification problems depending on the number of data points available, the sampling frequency, and the frequency range of interest.

7 Acknowledgement

The present research was partially supported by The Danish Technical Research Council within the project: **Dynamics of Structures**.

References

[1] Cecen, H., *Response of Ten Story, Reinforced Model Frames to Simulated Earthquakes.* Thesis presented to the University of Illinois, Urbana, Ill., in partial fulfillment of the requirements for the degree of Doctor of Philosophy, 1979.

[2] Daubechies, I., *Ten Lectures on Wavelets*

Society for Industrial and Applied Mathematics (SIAM), Philadelphia, Pa, 1992.

[3] DiPasquale, E. and Çakmak, A.S. *Seismic Damage Assessment using Linear Models.*, Soil Dynamics and Earthquake Engineering, Vol. 9, No. 4, pp. 194-215, 1990.

[4] Dipasquale, E. and Çakmak, A.S., Relation between Global Damage Indices and Local Stiffness Degradation

Journal of Structural Engineering, 1990, **116**, 5, 1440-56.

[5] Goupilland, P., Grossman, A. and Morlet, J., Cycle-Octave and Related Transforms in Seismic Signal Analysis

Geoexploration, Vol. 23, pp. 85-102.

[6] Mullen, C., Micaletti, R. C. and Çakmak, A. S. *A simple method for estimating the maximum softening damage index* Proc. of the 7th int. Conf. on Soil Dynamics and Structural Engineering

[7] Mallat, S.G., *A Theory for Multiresolution Signal Decomposition: The Wavelet Representation*

IEEE Transactions on Pattern Analysis and Machine Intelligence, Vol. 11, No. 7, 1989, pp. 674-93.

[8] Newland, D.E., *Random Vibrations, Spectral and Wavelet Analysis*

Longman, Harlow and John Wiley, New York, 3rd Edition, 1993.

[9] Rodriguez-Gomez, S., *Evaluation of Seismic Damage Indices for Reinforced Concrete Structures* M.Sc. Thesis, Princeton University, Oct. 1990.

STRUCTURAL RELIABILITY THEORY SERIES

PAPER NO. 114: H. U. Köylüoğlu & S. R. K. Nielsen: *Stochastic Dynamics of Linear Structures with Random Stiffness Properties and Random Damping subject to Random Loading.* ISSN 0902-7513 R9308.

PAPER NO. 115: H. U. Köylüoğlu & S. R. K. Nielsen: *New Approximations for SORM Integrals.* ISSN 0902-7513 R9303.

PAPER NO. 116: H. U. Köylüoğlu, S. R. K. Nielsen & A. Ş. Çakmak: *Stochastic Dynamics of Geometrically Non-Linear Structures subject to Stationary Random Excitation.* ISSN 0902-7513 R9418.

PAPER NO 117: H. U. Köylüoğlu, S. R. K. Nielsen & A. Ş. Çakmak: *Perturbation Solutions for Random Linear Structural Systems subject to Random Excitation using Stochastic Differential Equations.* ISSN 0902-7513 R9425.

PAPER NO. 118: I. Enevoldsen & J. D. Sørensen: *Reliability-Based Optimization in Structural Engineering.* ISSN 0902-7513 R9332.

PAPER NO. 119: I. Enevoldsen & K. J. Mørk: *Effects of a Vibration Mass Damper in a Wind Turbine Tower.* ISSN 0902-7513 R9334.

PAPER NO. 120: C. Pedersen & P. Thoft-Christensen: *Interactive Quasi-Newton Optimization Algorithms.* ISSN 0902-7513 R9346.

PAPER NO. 121: H. U. Köylüoğlu, S. R. K. Nielsen & A. Ş. Çakmak: *Applications of Interval Mapping for Structural Uncertainties and Pattern Loadings.* ISSN 0902-7513 R9411.

PAPER NO. 122: H. U. Köylüoğlu, S. R. K. Nielsen & A. Ş. Çakmak: *Fast Cell-to-Cell Mapping (Path Integration) with Probability Tails for the Random Vibration of Nonlinear and Hysteretic Systems.* ISSN 0902-7513 R9410.

PAPER NO. 123: A. Aşkar, H. U. Köylüoğlu, S. R. K. Nielsen & A. Ş. Çakmak: *Faster Simulation Methods for the Nonstationary Random Vibrations of Nonlinear MDOF Systems.* ISSN 0902-7513 R9405.

PAPER NO. 125: H. I. Hansen, P. H. Kirkegaard & S. R. K. Nielsen: *Modelling of Deteriorating RC-Structures under Stochastic Dynamic Loading by Neural Networks.* ISSN 0902-7513 R9409.

PAPER NO. 126: H. U. Köylüoğlu, S. R. K. Nielsen & A. Ş. Çakmak: *Reliability Approximations for MDOF Structures with Random Properties subject to Random Dynamic Excitation in Modal Subspaces.* ISSN 0902-7513 R9440.

PAPER NO. 128: H. U. Köylüoğlu, S. R. K. Nielsen, A. Ş. Çakmak & P. H. Kirkegaard: *Prediction of Global and Localized Damage and Future Reliability for RC Structures subject to Earthquakes.* ISSN 0901-7513 R9426.

PAPER NO. 129: C. Pedersen & P. Thoft-Christensen: *Interactive Structural Optimization with Quasi-Newton Algorithms.* ISSN 0902-7513 R9436.

STRUCTURAL RELIABILITY THEORY SERIES

PAPER NO. 130: I. Enevoldsen & J. D. Sørensen: *Decomposition Techniques and Effective Algorithms in Reliability-Based Optimization.* ISSN 0902-7513 R9412.

PAPER NO. 131: H. U. Köylüoğlu, S. R. K. Nielsen & A. Ş. Çakmak: *Approximate Forward Difference Equations for the Lower Order Non-Stationary Statistics of Geometrically Non-Linear Systems subject to Random Excitation.* ISSN 0902-7513 R9422.

PAPER NO. 132: I. B. Kroon: *Decision Theory applied to Structural Engineering Problems.* Ph.D.-Thesis. ISSN 0902-7513 R9421.

PAPER NO. 134: H. U. Köylüoğlu, S. R. K. Nielsen & A. Ş. Çakmak: *Solution of Random Structural System subject to Non-Stationary Excitation: Transforming the Equation with Random Coefficients to One with Deterministic Coefficients and Random Initial Conditions.* ISSN 0902-7513 R9429.

PAPER NO. 135: S. Engelund, J. D. Sørensen & S. Krenk: *Estimation of the Time to Initiation of Corrosion in Existing Uncracked Concrete Structures.* ISSN 0902-7513 R9438.

PAPER NO. 136: H. U. Köylüoğlu, S. R. K. Nielsen & A. Ş. Çakmak: *Solution Methods for Structures with Random Properties subject to Random Excitation.* ISSN 0902-7513 R9444.

PAPER NO. 137: J. D. Sørensen, M. H. Faber & I. B. Kroon: *Optimal Reliability-Based Planning of Experiments for POD Curves.* ISSN 0902-7513 R9455.

PAPER NO. 138: S.R.K. Nielsen & P.S. Skjærbæk, H.U. Köylüoğlu & A.Ş. Çakmak: *Prediction of Global Damage and Reliability based upon Sequential Identification and Updating of RC Structures subject to Earthquakes.* ISSN 0902-7513 R9505.

PAPER NO. 139: R. Iwankiewicz, S. R. K. Nielsen & P. S. Skjærbæk: *Sensitivity of Reliability Estimates in Partially Damaged RC Structures subject to Earthquakes, using Reduced Hysteretic Models.* ISSN 0902-7513 R9507.

PAPER NO. 142: S. R. K. Nielsen & R. Iwankiewicz: *Response of Non-Linear Systems to Renewal Impulses by Path Integration.* ISSN 0902-7513 R9512.

PAPER NO. 147: R. C. Micaletti, A. Ş. Çakmak, S. R. K. Nielsen & P. H. Kirkegaard: *Construction of Time-Dependent Spectra using Wavelet Analysis for Determination of Global Damage.* ISSN 0902-7513 R9517.

PAPER NO. 149: P. S. Skjærbæk, S. R. K. Nielsen & A. Ş. Çakmak: *Damage Location of Severely Damaged RC-Structures based on Measured Eigenperiods from a Single Response.* ISSN 0902-7513 R9518.

Department of Building Technology and Structural Engineering
Aalborg University, Sohngaardsholmsvej 57, DK 9000 Aalborg
Telephone: +45 98 15 85 22   Telefax: +45 98 14 82 43